07;08;13

Conductivity of nanocontact to $A^{III}As$- and $A^{III}Sb$ semiconductors with a native oxide layer

© P.A. Alekseev[1], E.V. Kunitsyna[1], V.S. Suntsova[1], A.N. Baranov[2], V.V. Romanov[1], K.D. Moiseev[1]

[1] Ioffe Institute, St. Petersburg, Russia
[2] Institute of Electronics and Systems, University of Montpellier/CNRS, Montpellier, France
E-mail: npoxep@gmail.com

Received December 7, 2023
Revised February 14, 2024
Accepted March 9, 2024

The work examines surface electronic phenomena in $A^{III}B^{V}$ semiconductors, namely $A^{III}As$ and $A^{III}Sb$ with a native oxide layer, using scanning probe microscopy methods. Using the Kelvin probe microscopy method, it was shown that the work function of a semiconductor is determined by the work function of the near-surface layer of a V-group element (As, Sb) formed during oxidation. Measurement of current-voltage characteristics using conductive atomic force microscopy revealed that the conductivity in the region of a point nanocontact is determined by the spreading resistance and the height of the Schottky barrier, which depends on the position of the Fermi level in the bulk of the semiconductor and the work function of the surface layer.

Keywords: $A^{III}B^{V}$, antimonides, arsenides, surface conductivity, native oxide, I-V curves.

DOI: 10.61011/TPL.2024.06.58477.19830

$A^{III}B^{V}$ semiconductors are used to construct electronic and optoelectronic devices; $A^{III}As$ and $A^{III}Sb$ compounds are applied in the design of devices operated in visible and infrared ranges. The efficiency of diode semiconductor structures depends largely on the magnitude of leakage currents under reverse bias. The surface is a major leakage path [1]. Our knowledge of the mechanism of surface conductivity is still incomplete. Surface conductivity provides an opportunity to fabricate Ohmic contacts to semiconductor materials. For example, owing to a high density of surface electron states, pinning of the Fermi level in the conduction band is observed in *n*- and *p*-InAs. This Fermi level pinning induces the emergence of a surface leakage path; a metal contact to such a surface is Ohmic and independent of the work function of the metal [2]. In GaSb, the surface Fermi level is pinned close to the valence band top. Therefore, the Schottky barrier for *p*-GaSb is significantly lower than the one for *n*-GaSb [3].

It has recently been demonstrated for $A^{III}As$ compounds that an As layer is emerged at the interface with a semiconductor crystal in the process of formation of a surface native oxide [4]. This layer acts as a source of surface electron states, and the effective work function model may be used to characterize Fermi level pinning on the surface [5]. The mentioned layer is also highly conductive; since the work function of As is lower than the electron affinity in InAs, an energy barrier between an As layer and a semiconductor is lacking. This provides an explanation for the Ohmic nature of contacts and the high surface conductivity. When the concentration of Al or Ga in AlInAs or InGaAs ternary solutions increases, the conduction band (electron affinity) shifts to a level above the work function of an As layer, a surface space charge region (SCR) forms, and the contact to a semiconductor becomes rectifying [6]. We have demonstrated earlier that, as in the case of arsenides, an Sb layer is emerged at the interface with a crystal in $A^{III}Sb$ compounds in the process of formation of a native oxide. It has been found that the work function of various $A^{III}Sb$ compounds is governed by the work function of Sb [7]. Thus, the effective work function model [5] is applicable to $A^{III}Sb$ and $A^{III}As$ compounds, and the magnitude of surface band bending in the region of a metal contact is defined not by the work function of a metal, but by the relation between the Fermi level position in the bulk of a semiconductor and the work function of a layer of atomic Sb [8] or As.

As semiconductor devices continue to miniaturize, their surface/bulk ratio increases, and surface electron phenomena become dominant. In addition, contacts to such devices become nanosized. The aim of the present study is to examine the conductivity of a nanocontact to various $A^{III}Sb$ and $A^{III}As$ semiconductors with a native oxide layer and establish the relation between this conductivity and the work function of a semiconductor.

Scanning probe microscopy (SPM) techniques were used in the study. The work function was determined by Kelvin probe microscopy with the reference surface of a highly oriented pyrolytic graphite with a known work function [4,7]. NSG30/Pt (NT-MDT, Russia) probes with a conductive Pt coating were used. Current–voltage curves (I-V curves) were measured with DCP30 (NT-MDT, Russia) probes with a conductive coating of diamond heavily doped with boron. Their tip curvature radius was 100 nm. To measure I-V curves on the surface with a layer of poorly conductive native oxide, the probe needs to perforate this

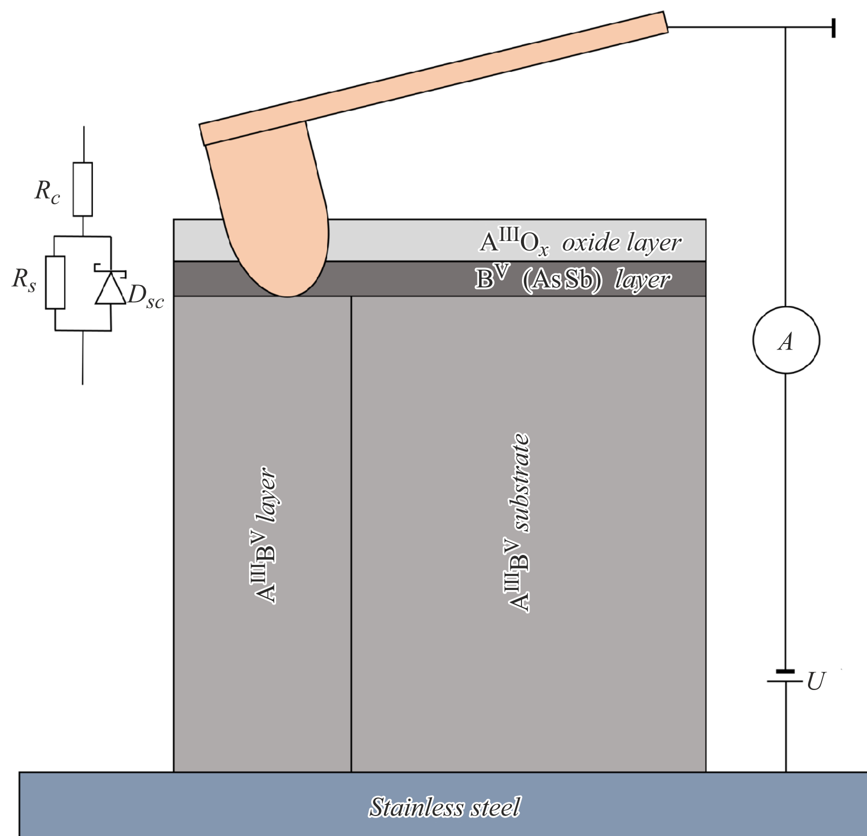

Figure 1. Measurement scheme of local I-V curves via conductive atomic force microscopy on the cleaved surface of a heterostructure with an oxide layer and a conductive layer of a group V element at the interface with a semiconductor. The equivalent electric circuit is shown on the left.

layer mechanically. A pressing force of $\sim 3\,\mu$N [9] was applied to the probe for this purpose.

Device $A^{III}Sb$ and $A^{III}As$ heterostructures were examined. The substrate with grown epitaxial layers was cleaved. Following cleavage, the structures were exposed to atmosphere for 24 h to form a surface oxide layer. These structures were then mounted with a conductive glue to a stainless steel holder in such a way that cleaved surface (110) was horizontal (Fig. 1).

It is important to emphasize that each layer had an electric contact to the holder. The cleaved surface was examined by SPM. Since the thickness of layers in the heterostructure exceeded $1\,\mu$m, the probe provided an opportunity to measure I-V curves and the surface potential of each individual layer (see the scheme in Fig. 1). The compositions and types and levels of doping of the studied samples are presented in the table.

Figure 2 presents the band diagrams [10], work functions, and bandgap edges for various semiconductor compounds. Circles denote the values measured in the present study, while squares correspond to literature data. It follows from Fig. 2 that the work function agrees with known values of 4.85 ± 0.15 eV for $A^{III}As$ [4] and 4.65 ± 0.10 eV for $A^{III}Sb$ [7]. Notably, the work function of *n*-type semiconductors is normally lower than the work function of *p*-type ones, and the difference increases with bandgap width, reaching a level of 0.2 eV [11]. This is apparently attributable to the thinness of the surface layer of a group V element and incomplete screening of the Fermi level position in the bulk of a doped semiconductor. It is of interest to note that the work function of $GaAs_{0.71}Sb_{0.29}$ lies between the values for *p*-GaAs and *p*-GaSb. The likely cause of this is the work function of an AsSb layer.

Figure 3 shows the I-V curves measured for various $A^{III}Sb$ and $A^{III}As$ semiconductors. The data for currents no greater than $1\,\mu$A are presented. At large currents, the nanocontact region may be heated significantly, making it difficult to interpret the experimental data correctly. It should be noted that the I-V curves for *p*-GaSb, *p*-$GaAs_{0.06}Sb_{0.94}$, *p*-$Ga_{0.78}In_{0.22}As_{0.18}Sb_{0.82}$, InAs, and an Au film 100 nm in thickness (shown for comparison) were linear with a slope corresponding to a resistance within the $8-20\,\mathrm{k}\Omega$ range. This is the resistance of a point contact (R_c). Changes in the contact area (due to differences in semiconductor surface roughness) and the oxide thickness lead to variations of the contact resistance. With the probe curvature radius taken into account, the contact resistance does not exceed $2 \cdot 10^{-6}\,\Omega \cdot \mathrm{cm}^{-2}$, which corresponds to the resistance of Ohmic micro- and macrocontacts [12]. Thus, the contact for relatively narrow-gap *p*-type $A^{III}Sb$

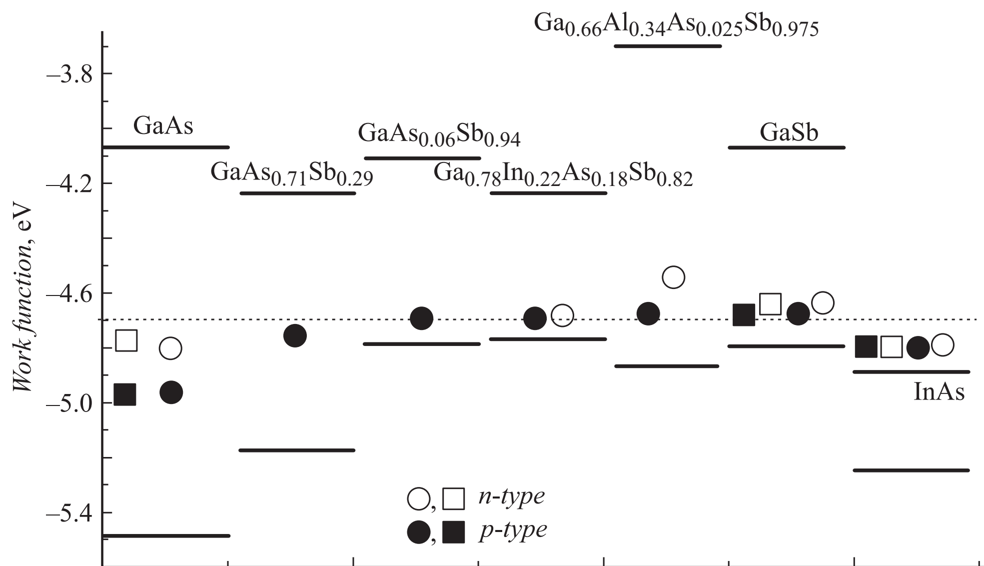

Figure 2. Work functions and band diagrams [10] of various A^{III}Sb and A^{III}As semiconductors. Circles represent the values measured in the present study, while squares correspond to literature data [2,11]. Filled and open symbols correspond to *p*- and *n*-type materials, respectively.

semiconductors is Ohmic. The band diagrams in Fig. 2 and the electric circuit in Fig. 1 may provide an explanation for this. When a mechanical contact to a semiconductor with a conductive layer of a group V element forms, one may identify three major circuit elements: point contact resistance R_c, spreading resistance R_s, and Schottky diode D_{sc}. The spreading resistance is set by the specific conductivity of a semiconductor and the contact area. Owing to the surface layer conductivity, the effective contact area may exceed the area of probe–surface contact. It is also important to note that the specific conductivity of a semiconductor depends on the magnitude of surface band bending. When an accumulation layer forms, the conductivity increases; when an SCR (depletion region) forms, the conductivity decreases.

The Schottky barrier is forward- or reverse-connected depending on the conductivity type of a semiconductor. The differential resistance of the Schottky diode depends on the parameters of a surface SCR that are specified by the difference between the Fermi level positions in the bulk of a semiconductor and on the surface (work function of the surface layer of a group V element), the doping level, and the carrier mobility. The work function on the surface of *p*-type A^{III}Sb semiconductors is indeed close to the Fermi level energy in the bulk of a semiconductor. Therefore, surface band bending is virtually nonexistent in these semiconductors, and this results in the formation of an Ohmic contact.

When the concentration of As or Al increases, the Fermi level in the bulk of a *p*-type semiconductor shifts downward, increasing the magnitude of surface band bending and making I-V curves nonlinear. For example, a nonlinear I-V curve with a spreading resistance of $2\,\mathrm{M\Omega}$ is observed for $Ga_{0.66}Al_{0.34}As_{0.025}Sb_{0.975}$. The I-V curve for $GaAs_{0.71}Sb_{0.29}$ is rectifying with a spreading resistance of $5\,\mathrm{G\Omega}$. A further enhancement of surface band bending in GaAs leads to currents $< 100\,\mathrm{pA}$ within the voltage interval from -2 to $2\,\mathrm{V}$.

I-V curves for *n*-type A^{III}Sb semiconductors are rectifying. The change in polarity of forward and reverse branches relative to that of rectifying I-V curves for *p*-type materials (cf. the I-V curves for *n*-GaSb and *p*-$GaAs_{0.71}Sb_{0.29}$) is evident. It is interesting to note that spreading resistance R_s for *n*-$Ga_{0.66}Al_{0.34}As_{0.025}Sb_{0.975}$ is $1.5\,\mathrm{M\Omega}$, which is close to the R_s value for an *p*-type semiconductor of the same composition. The spreading resistance for *n*-$Ga_{0.78}In_{0.22}As_{0.18}Sb_{0.82}$ is $6\,\mathrm{M\Omega}$, while *n*-GaSb has $R_s = 100\,\mathrm{M\Omega}$. The difference in spreading resistance values may be attributed qualitatively to different levels of doping of semiconductors and to variations of the magnitude of band bending that affects the specific conductivity. In addition, the effective contact area may increase due to thickening of the conductive layer in the process of formation of a native oxide. It should be taken into account the thicker native oxide, the thicker conductive layer grows [4]. In the case of ternary and quaternary solid solutions with added In and Al, the surface oxide thickness is higher [4,13]. in addition, the conductivity of amorphous As [14] is several orders of magnitude lower than the conductivity of amorphous Sb [15].

Thus, the values of work function on surface (110) of A^{III}Sb and A^{III}As semiconductors with a native oxide layer were measured. It was demonstrated that the work function is $4.85 \pm 0.15\,\mathrm{eV}$ for A^{III}As and $4.65 \pm 0.10\,\mathrm{eV}$ for A^{III}Sb. The work function is governed by the work function of a group V element that forms a surface conductive layer in

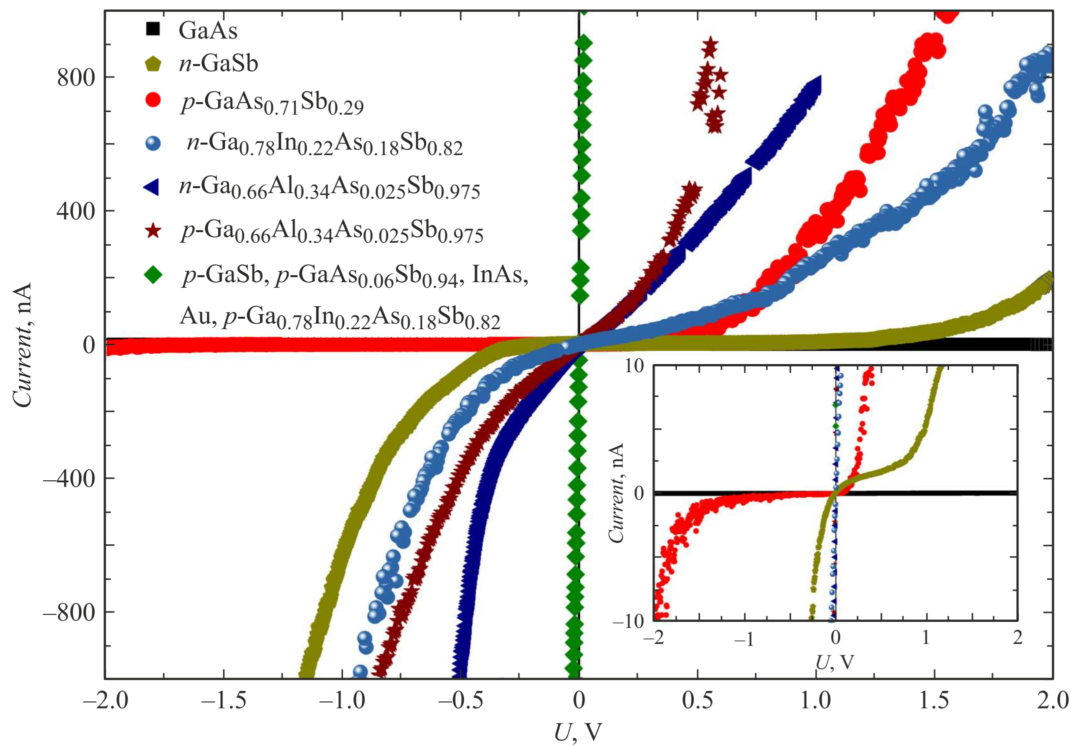

Figure 3. I-V curves measured on contact of the SPM probe with various $A^{III}Sb$ and $A^{III}As$ semiconductors.

Type and level (cm^{-3}) of doping of the examined semiconductor materials

GaAs	InAs	GaSb	$GaAs_{0.71}Sb_{0.29}$	$GaAs_{0.06}Sb_{0.94}$	$Ga_{0.78}In_{0.22}As_{0.18}Sb_{0.82}$	$Ga_{0.66}Al_{0.34}As_{0.025}Sb_{0.975}$
n, 10^{18} p, 10^{18}	n, 10^{18} p, 10^{18}	n, 10^{17} p, 10^{17}	p, 10^{16}	p, 10^{16}	n, 10^{17} p, 10^{17}	n, 10^{18} p, 10^{18}

the course of oxidation. When a nanocontact to the surface of a semiconductor is formed, the conductivity is set by the spreading resistance and the magnitude of surface band bending between the layer and the semiconductor material. The obtained results should help design $A^{III}Sb$ and $A^{III}As$ devices with improved performance features.

Funding

This study was supported by grant No. 22-22-00121 from the Russian Science Foundation (https://rscf.ru/project/22-22-00121/).

Conflict of interest

The authors declare that they have no conflict of interest.

References

[1] B. Marozas, W. Hughes, X. Du, D. Sidor, G. Savich, G. Wicks, Opt. Mater. Express, **8** (6), 1419 (2018). DOI: 10.1364/OME.8.001419

[2] H.-U. Baier, L. Koenders, W. Mönch, Solid State Commun., **58** (5), 327 (1986). DOI: 10.1016/0038-1098(86)90094-3

[3] K. Nishi, M. Yokoyama, S. Kim, H. Yokoyama, M. Takenaka, S. Takagi, J. Appl. Phys., **115** (3), 034515 (2014). DOI: 10.1063/1.4862486

[4] P.A. Alekseev, M.S. Dunaevskiy, G.E. Cirlin, R.R. Reznik, A.N. Smirnov, D.A. Kirilenko, V.Y. Davydov, V.L. Berkovits, Nanotechnology, **29** (31), 314003 (2018). DOI: 10.1088/1361-6528/aac480

[5] J. Freeouf, J. Woodall, Appl. Phys. Lett., **39** (9), 727 (1981). DOI: 10.1063/1.92863

[6] P.A. Alekseev, V.A. Sharov, M.S. Dunaevskiy, D.A. Kirilenko, I.V. Ilkiv, R.R. Reznik, G.E. Cirlin, V.L. Berkovits, Nano Lett., **19** (7), 4463 (2019). DOI: 10.1021/acs.nanolett.9b01264

[7] P.A. Alekseev, A.N. Smirnov, V.A. Sharov, B.R. Borodin, E.V. Kunitsyna, Bull. Russ. Acad. Sci. Phys., **87** (6), 728 (2023). DOI: 10.3103/S1062873823702040.

[8] P.A. Alekseev, I.A. Eliseyev, V.V. Romanov, K.D. Moiseev, E.V. Kunitsyna, B.R. Borodin, V.A. Sharov, A.N. Smirnov, V.Yu. Davydov, Appl. Phys. Lett., **123** (26), 261601 (2023). DOI: 10.1063/5.0164062

[9] B.R. Borodin, P.A. Alekseev, V. Khayrudinov, E. Ubyivovk, Yu. Berdnikov, N. Sibirev, H. Lipsanen, CrystEngComm, **25** (9), 1374 (2023). DOI: 10.1039/D2CE01438F
[10] V.V. Romanov, K.D. Moiseev, T.I. Voronina, T.S. Lagunova, Yu.P. Yakovlev, Semiconductors, **42** (12), 1403 (2008). DOI: 10.1134/S1063782608120051.
[11] W.E. Spicer, I. Lindau, P. Skeath, C.Y. Su, P. Chye, Phys. Rev. Lett., **44** (6), 420 (1980). DOI: 10.1103/PhysRevLett.44.420
[12] T.V. Blank, Yu.A. Gol'dberg, Semiconductors, **41** (11), 1263 (2007). DOI: 10.1134/S1063782607110012.
[13] P. Dementyev, M. Dunaevskii, A. Ankudinov, I. Makarenko, V. Petrov, A. Titkov, A. Baranov, D. Yarekha, R. Laiho, Appl. Phys. Lett., **89** (8), 081103 (2006). DOI: 10.1063/1.2338002
[14] G. Greaves, S. Elliott, E. Davis, Adv. Phys., **28** (1), 49 (1979). DOI: 10.1080/00018737900101355
[15] J. Hauser, Phys. Rev. B, **9** (6), 2623 (1974). DOI: 10.1103/PhysRevB.9.2623

Translated by D.Safin